

## THE EFFECTS OF VOLUTE DESIGN PARAMETERS ON THE PERFORMANCE OF A CENTRIFUGAL PUMP

**Ayhan Nazmi İlikan**

Dr.

TÜBİTAK Rail Transportation Technologies  
Institute

ayhan.ilikan@tubitak.gov.tr

**Erkan Ayder**

Prof. Dr.

İTÜ Faculty of Mechanical Engineering  
aydere@itu.edu.tr

### ABSTRACT

The volute, one of the centrifugal pump components, creates uniform circumferential conditions at the impeller outlet, serving the function of collecting the fluid. The volute's geometry is designed to increase the cross-sectional area from the impeller outlet to the pump discharge flange. Parameters such as the rate of increase in cross-sectional area, cross-sectional shape, and the angle of the section relative to the pump axis play a role in volute design. In this study, a centrifugal pump impeller and volute were designed, taking a commercially available product as a reference. The designed pump has a rated flow rate of 125 m<sup>3</sup>/h, a head of 20 m, and a speed of 1450 rpm, and it is used as a water pump. Computational Fluid Dynamics (CFD) simulations were conducted using the reference design as a basis. After verifying the reference design with the CFD method, simulations continued on the volute by modifying volute design parameters. The performance of the volute geometry was examined by changing the cross-section to be circular, left-leaning asymmetric, right-leaning asymmetric, and trapezoidal. The calculations were carried out under three-dimensional, steady-state, turbulent flow conditions, using a hexahedral grid. The volute's pressure loss and static pressure recovery coefficients were obtained along the pump performance curve. During the calculations, the volute outlet pressure and tangential velocity at the inlet were kept constant while changing the radial velocity, i.e., the water flow rate, and the inlet angle. The distribution of velocity and pressure fields within the volute was examined through contours. The study concluded that the volute's cross-sectional shape has a significant impact, especially around the design flow rate, and the best performance is achieved with a symmetric circular cross-sectional volute.

### INTRODUCTION

Centrifugal pump volute design is supported by numerous methods in the literature, frequently utilized by designers such as those developed by Eckert and Schnell [1], Pfleiderer [2], Stepanoff [3], and Troskolanski and Lazarkiewicz [4]. Moreover, new methods derived from Computational Fluid

Dynamics (CFD) have also been documented [5]. With the widespread adoption of CFD methods in the past quarter-century, the design steps for pump volutes have increasingly relied on CFD, leading to numerous publications in this area [6, 7]. Knapp et al. [8] compared the Pfleiderer and Stepanoff methods, both established in the literature, for designing a circular-section volute using the CFD method, examining their effects on pump performance. The study emphasized that altering the volute geometry design method presents an opportunity to enhance pump efficiency. Chan et al. [9] compared the constant angular momentum and constant mean velocity methods in volute design using CFD. Simulation results showed that the volute designed using the constant angular momentum method outperformed the other method in terms of radial force magnitude and peak scalar stresses for a fixed head value. To achieve optimal results, the study highlighted the necessity of surpassing traditional experimental methods in volute design. Yang et al. [10] investigated the effects of variations in volute cross-sectional area shape, cross-sectional change method, and the gap between the pump impeller and volute tongue on pump performance using the CFD method. Circular, horseshoe, trapezoidal, and rectangular sections were examined, with the circular section volute yielding the best performance. Jin et al. [11] examined the effects of altering volute section areas by changing from the standard model by increasing the section area by 10% through time-dependent CFD analyses, particularly noting the superior performance of the modified geometry, especially at low flow rates. Chen et al. [12] used the CFD method to optimize the efficiency of a dual-suction pump impeller and volute pair by parametrically altering volute section parameters, reducing fluctuations in head by 40%. Van den Braembussche [13] highlighted in their report that the flow within the volute is equally dependent on the flow conditions at the impeller outlet as it is on the volute geometry, stressing the necessity of optimizing both the impeller and volute together to achieve minimum radial velocity at the impeller outlet. Similarly, Ayder [14] demonstrated through experimental studies on three-dimensional volute geometries that the flow impacting the outer surface of the volute induces vortex formation, dominating the

flow differently from two-dimensional volute flow. They noted that the vortex intensity is proportional to the radial velocity at the volute inlet, indicating more intense vortex movement at higher flow rates. Regarding section geometry, they mentioned that methods defining the flow within the volute in 3D assume the flow to be axisymmetric, limiting their use to circular-section volute.

The literature review outlined above reveals numerous studies on pump volutes, particularly after the widespread adoption of CFD methods. However, a study focusing solely on altering the section shape of volute while keeping all other parameters constant, and directly examining the volute's performance without involving the impeller and maintaining constant conditions at the volute inlet, has not been encountered. In this study,  $V_r/V_t$  inlet conditions were defined at the volute-pump impeller interface, and the performance of the volute was directly examined. Volute sections were altered to be circular, right-leaning asymmetric, left-leaning asymmetric, and trapezoidal, and performance curves were obtained. Subsequently, sections were taken at various positions to examine differences in flow structure among volutes with different section geometries.

## SYMBOLS

- b2: Impeller outlet width (mm)
- $C_p$ : Static pressure recovery coefficient
- $D_s$ : Suction flange diameter (mm)
- $D_d$ : Discharge flange diameter (mm)
- $D_i$ : Pump impeller diameter (mm)
- $G_s$ : Pump shaft power (kW)
- H: Pump head (m)
- n: Pump impeller rotational speed (rpm)
- $\eta$ : Pump hydraulic efficiency
- $P_i$ : Volute inlet pressure (bar)
- $P_o$ : Volute outlet pressure (bar)
- Q: Pump volumetric flow rate (m<sup>3</sup>/h)
- $\omega$ : Total pressure loss coefficient
- $\circ$ : Total pressure exponent

## IMPELLER AND VOLUTE DESIGN

For the investigation of the effects of volute section geometry on pump performance, initially, a reference pump was required. This pump was selected from the centrifugal type water pumps in the catalog of a commercial pump manufacturer. The specifications of the relevant pump are presented in Table 1.

Firstly, a pump impeller and volute design with similar characteristics to the reference pump were created. CFTurbo commercial software was utilized during the design process. The design criteria targeted the nominal flow rate, head, and

speed of the reference pump. With these data, the specific speed  $nq$  was calculated as 29.

Table 1. The specifications of the reference pump

Parameter	Value
n	1450 rpm
Q	125 m <sup>3</sup> /h
H	19.9 m
$G_s$	8.55 kW
$\eta$	78.8 %
$D_s$	DN125
$D_d$	DN100
$D_i$	256 mm

The impeller diameter was determined by calculating the specific diameter from the Cordier diagram. After determining the dimensions based on the suction and discharge flange sizes of the reference pump, the volute design was implemented. Using the Pfleiderer method, the volute geometry was created to ensure that the product of the tangential velocity of the fluid at various sections and the distance from the impeller center remains constant. During the first volute design for validation, the position of the volute relative to the impeller, both in front and behind the impeller, was symmetrically determined with respect to the middle of the outlet surface defined by b2. The meridional and perspective views of the pump impeller and volute are provided in Figure 1.

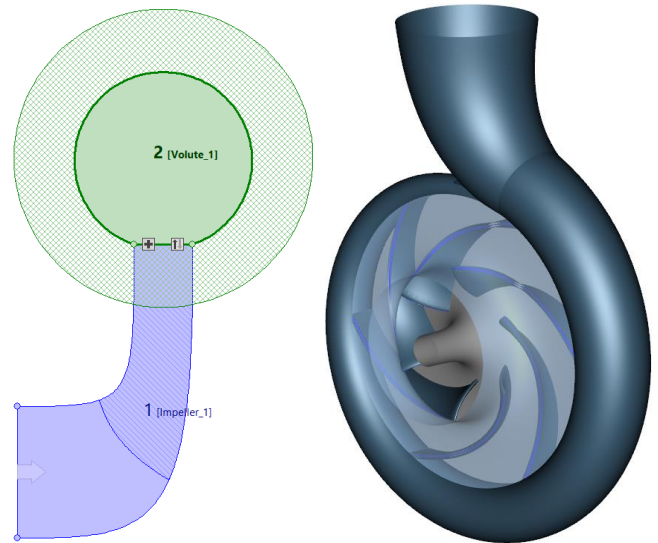


Figure 1. The meridional and perspective views of the designed pump impeller and volute

## GRID GENERATION AND NUMERICAL MODEL

After creating the impeller and volute geometries, the STAR-CCM+ Computational Fluid Dynamics (CFD) commercial software was utilized to check whether the pump performance met the desired criteria. Initially, calculations were conducted at the design flow rate. The modeling was performed in three dimensions under steady-state, turbulent flow conditions. Water with constant density under standard conditions was used as the fluid. The Moving Reference Frame (MRF) method was chosen to model the rotation of the impeller. The  $k-\epsilon$  Realizable turbulence model was selected, and the Two-Layer All  $y^+$  Wall Treatment model was used to model the boundary layer flow over solid surfaces. This allowed the  $k-\epsilon$  model to be valid even if the required  $y^+$  values on the surface were not achieved. The hybrid feature enabled appropriate modeling in coarse mesh regions with high  $y^+$  values and in fine mesh regions with low values. Hexahedral cells were used to construct the solution grid, and a boundary layer mesh was used near the solid surfaces of the impeller and volute where gradients are high to obtain accurate results. At the design flow rate, the inlet boundary condition for the pump impeller was defined as mass flow rate, while the outlet boundary condition for the volute was set to atmospheric pressure. Additionally, to account for possible recirculation at the pump outlet flange surface during the solution process, the flow volume was extended a certain distance from the volute outlet surface. Subsequently, the mesh density was varied to calculate the head, power, and efficiency values, and the mesh independence was determined. The values obtained from the mesh density study are provided in Table 2. The results showed minimal changes up to 1.5 million mesh cells, and no significant difference was observed between 1.5 million and 2 million mesh cells. Therefore, further analysis was conducted using the mesh settings providing a 1.5 million-cell grid. The visualization of the created mesh is shown in Figure 2.

Table 2. The results of the mesh density study

Number of cells	Cell size	Q	H	$G_s$	$\eta$
~500k	8 mm	125	19.3	7.64	0.86
~850k	6 mm	125	19.3	7.68	0.86
~1M	4 mm	125	18.5	7.75	0.81
~1.5M	3 mm	125	18.4	7.74	0.81
~2M	2 mm	125	18.4	7.75	0.81

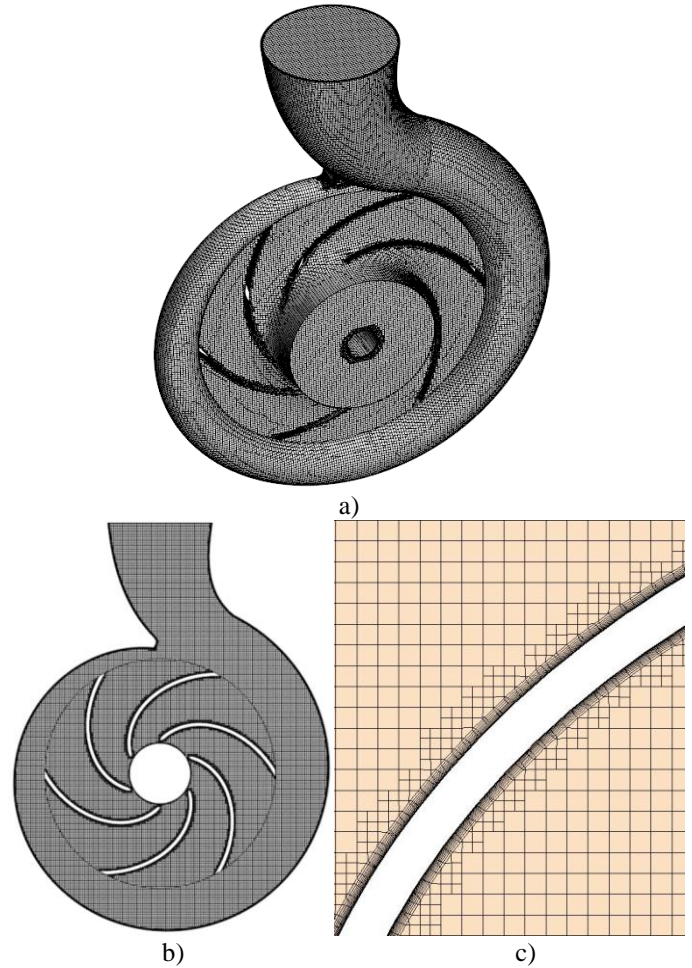


Figure 2. Solution grid a) 3D view, b) sectional view, c) boundary layer solution grid around the impeller blade

## PUMP CHARACTERISTIC CURVE

After determining the appropriate solution grid settings, the pump's characteristic curve was obtained. While the outlet static pressure was kept constant under atmospheric conditions, the inlet mass flow rate was varied at a constant speed to obtain pump performance parameters. The head and hydraulic efficiency characteristic curves obtained using the CFD method were compared with the curves found in the catalog of the commercial pump referenced at the beginning of the study. Upon examining the curves presented in Figure 3, it can be observed that the results are highly consistent, with an average error rate of around 5-8% in both the head and efficiency curves.

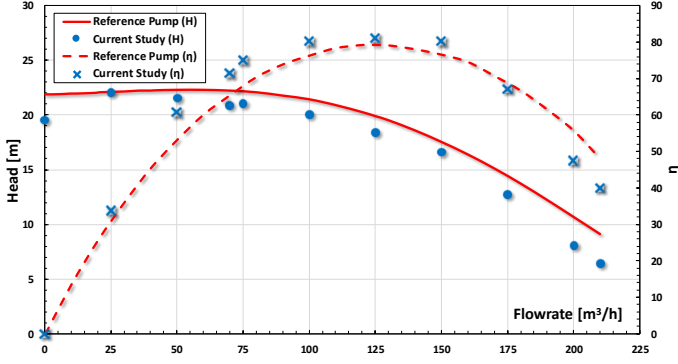


Figure 3. The performance curves of the reference and the designed pump

### CREATION OF VOLUTE SECTION GEOMETRIES

To investigate the effects of the volute section geometry, the pump impeller was removed from the model, and only the flow within the volute geometries was solved. Radial and tangential velocity components were defined as the inlet boundary conditions on the interface between the volute and the pump impeller, while the volute outlet was extended slightly to prevent reverse flow that could occur at the volute exit. Atmospheric pressure boundary conditions were applied at the outlet surface. During the analysis at various flow rates, the tangential velocity ( $V_t$ ) corresponding to the pump's nominal speed of 1450 rpm was kept constant at the volute inlet, while the radial velocity ( $V_r$ ) was varied. Additionally, to simplify the solution and focus on the effect of the volute section geometry, uniform flow conditions were assumed at the impeller-volute interface, and radial and tangential velocities were defined uniformly distributed over this surface. The performance of the volute, expressed in terms of the static pressure recovery coefficient ( $C_p$ ), total pressure loss coefficient ( $\omega$ ), and the ratio of inlet to outlet kinetic energies ( $V_r/V_t$ ), is defined as a function of these parameters according to Equations 1-3.

$$C_p = \frac{P_o - P_i}{P_i^o - P_i} \quad (1)$$

$$\omega = \frac{P_i^o - P_o^o}{P_i^o - P_i} \quad (2)$$

$$1 - (\omega + C_p) = \frac{P_o^o - P_o}{P_i^o - P_i} \quad (3)$$

The performance parameters of the volute were obtained for four different volute section geometries while keeping the outlet flange surface constant in diameter and circular in shape. The first volute, obtained in the validation study, has a circular section. As seen in Figure 4, the centerline of this volute section is aligned with the axis perpendicular to the impeller, and the volute section is symmetric with respect to the centerline. The next two volutes have circular and symmetric sections, one inclined towards the fluid inlet direction (left inclined) and the

other inclined towards the drive motor direction (right inclined) geometries. The final volute geometry differs from the first one only in that its section is trapezoidal instead of circular. Figure 5 shows the solid model views of the four volutes.

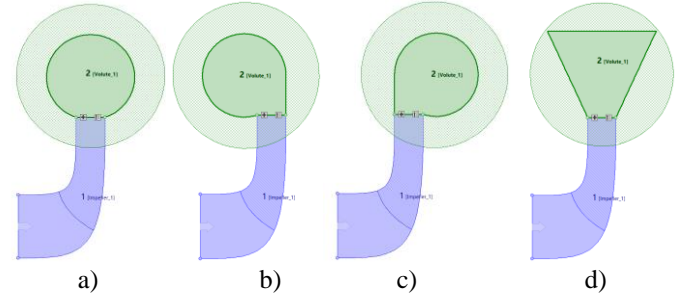


Figure 4. The meridional views of the volutes: a) circular, b) left inclined asymmetric, c) right inclined asymmetric, d) trapezoidal section

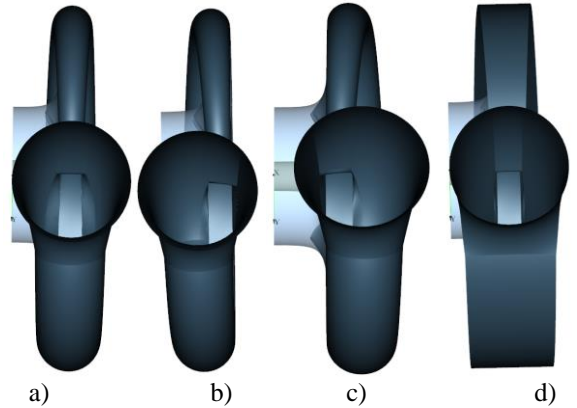


Figure 5. The solid model views of the volutes: a) circular, b) left inclined asymmetric, c) right inclined asymmetric, d) trapezoidal section

In Figure 6, the variation of the volutes' circumferential area with angle change can be observed. The section view and the section area increase curve in Figure 6 are the same for all four volutes. As mentioned earlier, in volute designs where the product of the fluid's tangential velocity and radius remains constant, the sections wrap around the impeller 360° in the circumferential direction, resulting in an approximately linear increase in section areas.

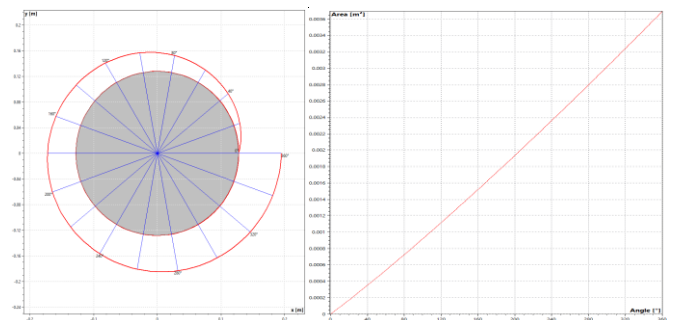


Figure 6. The circumferential changes in the areas of the volutes

The difference between the four volute section geometries can be seen in Figure 7. In each case, the volute exit section is circular and of the same size, while in the left and right inclined asymmetric volutes, the exit section is tangent to the outer surface (shroud) of the impeller. In the trapezoidal section volute, the cone angle is  $25^\circ$ .

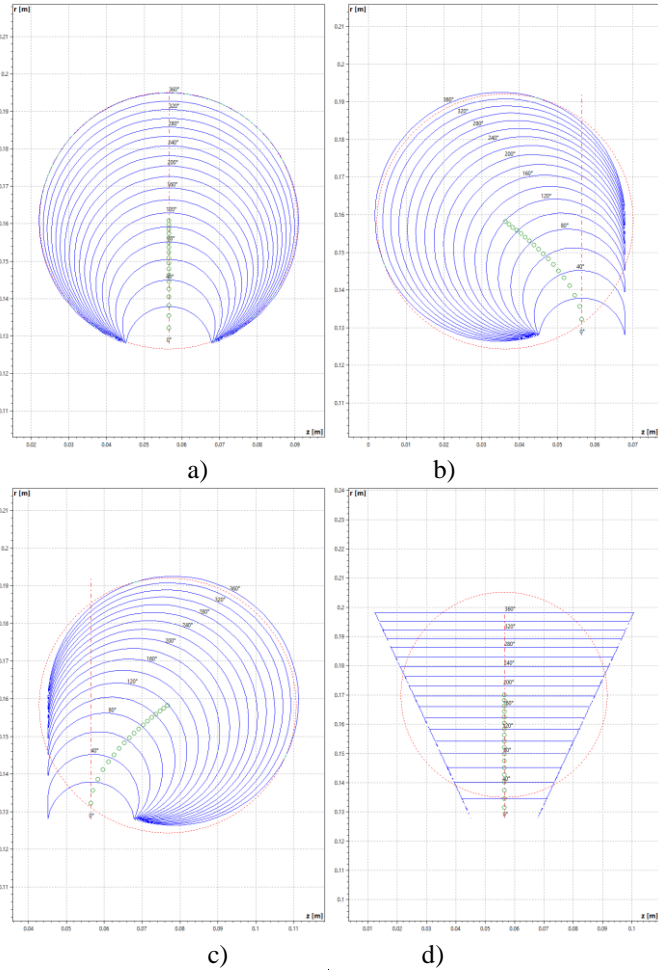


Figure 8. Views of the volute sections at various angles: a) circular, b) left inclined asymmetric, c) right inclined asymmetric, d) trapezoidal section

### THE EFFECT OF VOLUTE SECTION GEOMETRIES ON PERFORMANCE

The variation of volute performance parameters throughout the operating range is presented in Figures 8-10. The nominal operating flow rate of the pump corresponds to a  $V_r/V_t$  value of 0.16. When examining the static pressure recovery coefficient  $C_p$  curves, it is observed that the curves approach each other at values far from the nominal operating point. As the flow rates deviate from the design flow rate at low flow rates, resulting in increased pressure losses,  $C_p$  decreases. At high flow rates, despite the increase in cross-sectional area from inlet to outlet,  $C_p$  decreases to negative values due to the losses caused by high

velocity, indicating that the volute cannot increase the fluid pressure but decreases it.

The differences caused by the four different volute geometries are most pronounced around the nominal flow rate. In this region, the circular section provided the best performance, followed by the trapezoidal and left-right inclined sections. The performance of the left and right inclined curves remains the same throughout the operating range. Additionally, a sudden decrease in  $C_p$  is observed at values of  $V_r/V_t$  of 0.15 in the circular section volute and 0.17 in the inclined section volutes. This effect is more pronounced in the inclined geometries compared to the circular one, which is confirmed by the loss coefficient  $\omega$  given in Figure 9. The loss coefficient  $\omega$  is high in regions where  $C_p$  is low and low in regions where  $C_p$  is high.

Looking at the overall structure of the loss coefficient curves, it is observed that the least pressure loss is expected around the design flow rate for all curves. Regarding the effect of geometries, unlike  $C_p$ , there is higher loss in the trapezoidal curve at low flow rates compared to others, while at high flow rates, there is less total pressure loss in the circular section volute.

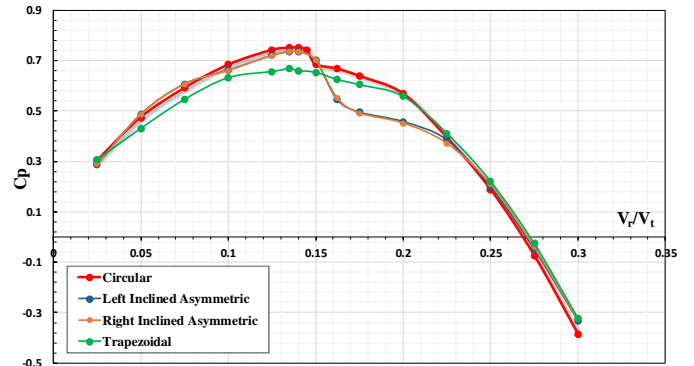


Figure 8. The variation of  $C_p$  with  $V_r/V_t$  for different volute sections

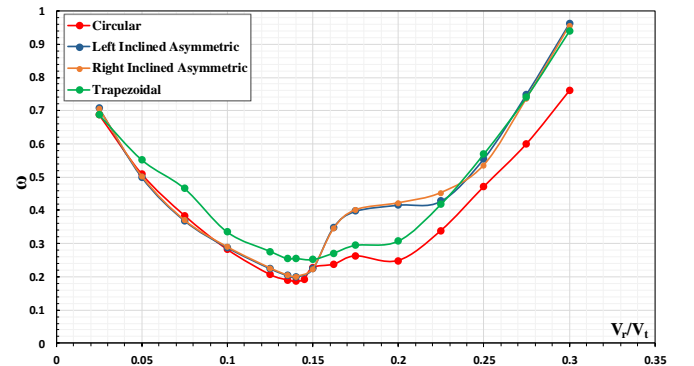


Figure 9. The variation of  $\omega$  with  $V_r/V_t$  for different volute sections

The difference in the total pressure loss at high flow rates, where it is lower in the circular section volute compared to

others, along with the consistency of  $C_p$ , results in noticeable differences in the outlet/inlet kinetic energy ratio curves shown in Figure 10. Particularly at flow rates higher than the design operating point, this ratio is higher in the circular section volute. The reason for this is that the low total pressure loss allows for more kinetic energy reserve to remain compared to other geometries.

Figure 11 shows the  $C_p$  contours obtained at the midsection of the volute at the design flow rate ( $V_r/V_t=0.16$ ). When examining the color scales, it can be observed that the  $C_p$  contours of the four geometries are quite similar almost up to the outlet of the volute. It is evident that the right and left inclined asymmetric volutes exhibit identical distributions throughout the entire section. While low-pressure zones are observed on the outer surfaces of these two geometries, they are considerably smaller in the trapezoidal and circular sections. A similar situation applies to the inner surface of the volute, namely the interface with the impeller. The reason for the lower  $C_p$  values in the right and left inclined asymmetric geometries can be explained by these regions.

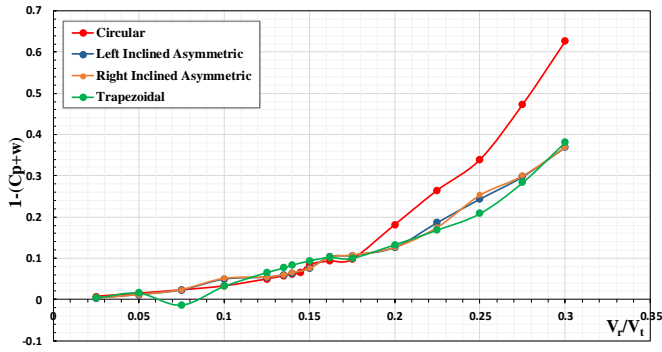


Figure 10. The variation of the outlet/inlet kinetic energy ratios with  $V_r/V_t$  for different volute sections

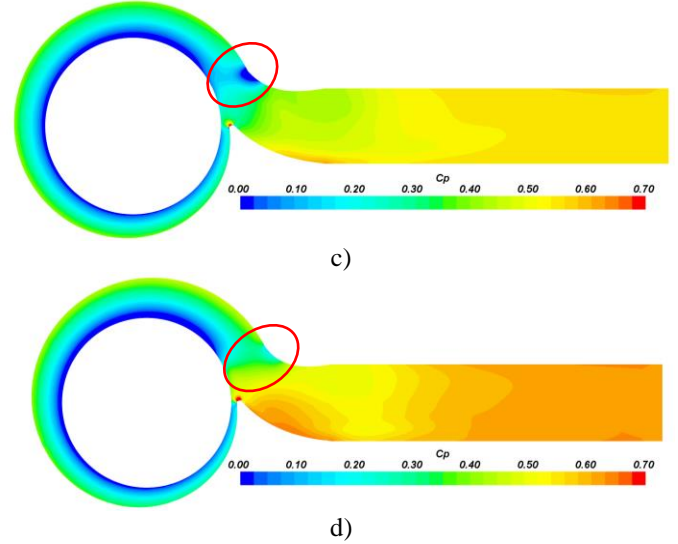
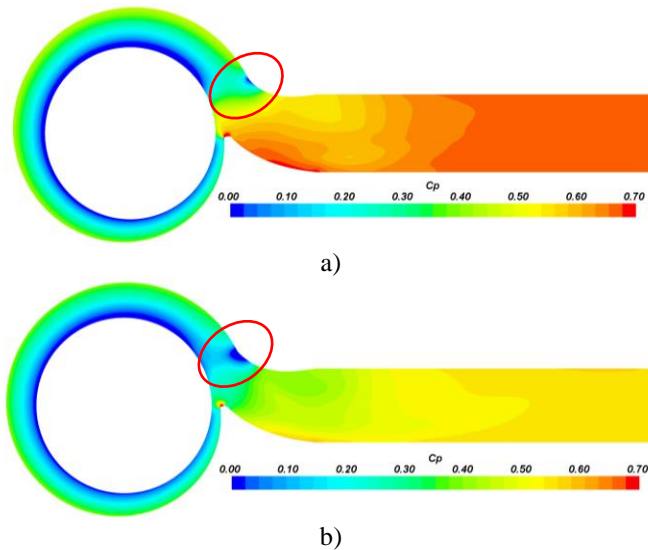


Figure 11. Local  $C_p$  contours on the mid-sections of the volutes at the design flow rate ( $V_r/V_t=0.16$ ): a) circular, b) left inclined asymmetric, c) right inclined asymmetric, d) trapezoidal section

In Figures 12-14, tangential velocity contours, namely the velocity perpendicular to the respective sections, are provided at  $330^\circ$ ,  $180^\circ$ , and  $90^\circ$ , respectively, at the design flow rate. As expected, in all three figures, contours for circular and trapezoidal geometries are symmetric with respect to the centerline of the volute. The contours for left and right inclined asymmetric geometries are symmetric with respect to each other.

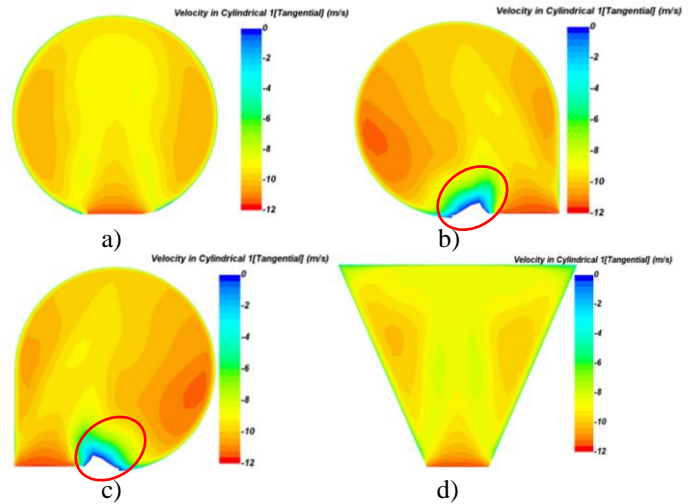


Figure 12. Contour plots of tangential velocity taken at sections at  $330^\circ$  in the circumferential direction at the design flow rate ( $V_r/V_t=0.16$ ): a) circular, b) left inclined asymmetric, c) right inclined asymmetric, d) trapezoidal section

Considering that the velocity scales are kept the same in all three figures, it can be said that the tangential velocity remains

approximately constant at all circumferential angles and for all geometries. This is because the design has been carried out accordingly. The low-pressure region observed on the inner surfaces of the left and right inclined asymmetric geometries in Figure 11 is also evident in Figure 12.

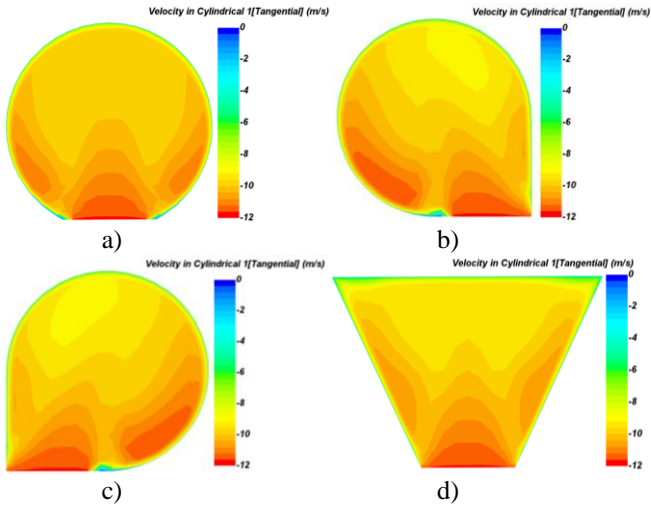


Figure 13. Contour plots of tangential velocity taken at sections at  $180^\circ$  in the circumferential direction at the design flow rate ( $V_r/V_t=0.16$ ): a) circular, b) left inclined asymmetric, c) right inclined asymmetric, d) trapezoidal section

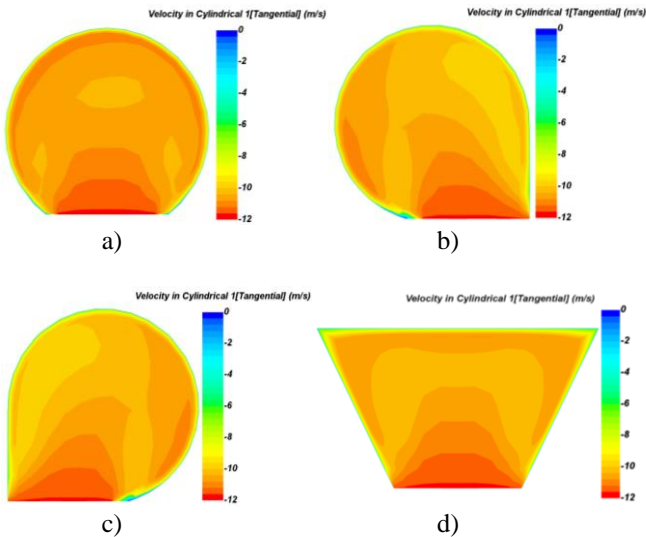


Figure 14. Contour plots of tangential velocity taken at sections at  $90^\circ$  in the circumferential direction at the design flow rate ( $V_r/V_t=0.16$ ): a) circular, b) left inclined asymmetric, c) right inclined asymmetric, d) trapezoidal section

## CONCLUSION

In this study, a centrifugal-type impeller and volute design were conducted with the assistance of CFD method, and

simulations were carried out. Performance analyses throughout the operating range of the geometry, including the impeller and volute pair, were performed to validate the model. Subsequently, the effect of volute section geometry was investigated by varying it to be circular, left inclined asymmetric, right inclined asymmetric, and trapezoidal shapes, again using CFD simulations. The following conclusions were drawn from the analysis results:

- Changes in section geometry did not significantly affect the static pressure recovery coefficient  $C_p$  in regions of very high or low flow rates compared to the design flow rate.

- The highest  $C_p$  value around the design flow rate was achieved with a circular section geometry.

- The lowest loss coefficient  $\omega$  around the design flow rate was obtained with a circular section volute in all section geometries.

- At flow rates higher than the design flow rate, the lower total pressure loss of the circular section volute allowed for a higher ratio of outlet to inlet kinetic energy compared to other geometries.

- A constant tangential velocity condition was maintained along the volute's circumferential direction for all section geometries, with the circular section volute providing the best performance.

## ACKNOWLEDGMENTS

The authors would like to thank TÜBİTAK Rail Transport Technologies Institute, CFTurbo GmbH, and Desica Design Machinery Trade and Industry Ltd. for their infrastructure support.

## REFERENCES

- 1.B. Eckert and E. Schnell, 1953, "Axial-und Radialkompressoren: Anwendung/Theorie/Berechnung", Berlin, Heidelberg: Springer-Verlag.
- 2.C. Pfeleiderer, 1955, "Die Kreiselpumpen für Flüssigkeit und Gase", 4th ed. Berlin, Heidelberg: Springer-Verlag.
- 3.A. J. Stepanoff, 1959, "Radial-und Axialpumpen-Theorie, Entwurf, Anwendung", Berlin, Heidelberg: Springer-Verlag.
- 4.A. T. Troskolanski and S. Lazarkiewicz, 1976, "Kreiselpumpen-Berechnung und Konstruktion", Basel und Stuttgart: Birkhauser Verlag.
- 5.T. Wang, H. Yu, Y. Fang, R. Xiang, N. Kan, and J. Yan, 2022, "A new design for energy-saving volutes in centrifugal pumps," Physics of Fluids, vol. 34, no. 11, p. 115119, doi: 10.1063/5.0122684.
- 6.J. H. Kim, K. T. Oh, K. B. Pyun, C. K. Kim, Y. S. Choi, and J. Y. Yoon, 2012, "Design optimization of a centrifugal pump impeller and volute using computational fluid dynamics," IOP Conference Series: Earth and Environmental Science, vol. 15, no. 3, p. 032025, doi: 10.1088/1755-1315/15/3/032025.
- 7.K. S. Cho, A. T. an, and S. M. Thu, 2019, "Design of Centrifugal Pump Volute-Type Casing," International Journal of

Science and Engineering Applications, vol. 8, no. 8, pp. 325–330.

8. A. Knapp, M. Böhle, and H. Roclawski, 2017, "Investigation of different design methods of volutes with circular cross sections for a single-stage centrifugal pump".

9. W. K. Chan, Y. W. Wong, and W. Hu, 2005, "Design Considerations of Volute Geometry of a Centrifugal Blood Pump," *Artif Organs*, vol. 29, no. 12, pp. 937–948.

10. S. Yang, F. Kong, and B. Chen, 2011, "Research on Pump Volute Design Method Using CFD," *International Journal of Rotating Machinery*, vol. 2011, p. 137860, doi: 10.1155/2011/137860.

11. H. B. Jin, M. J. Kim, and W. J. Chung, 2018, "A Study on the Effect of Variation of the Cross-sectional Area of Spiral Volute Casing for Centrifugal Pump." Zenodo, doi: 10.5281/zenodo.1082123.

12. S. Y. Chen, L. Zhang, Y. Sekino, and H. Watanabe, 2019, "Effects of Volute Cross-Sectional Area Distribution on Performance of Double-Suction Volute Pump," in *AJKFluids2019*, Volume 3B: Fluid Applications and Systems, Jul. 2019. doi: 10.1115/AJKFluids2019-5251.

13. R. Van den Braembussche, 2006, "Flow and Loss Mechanisms in Volute of Centrifugal Pumps," p. 27.

14. E. Ayder, 1993, "Experimental and Numerical Analysis of The Flow In Centrifugal Compressor and Pump Volutes," Universiteit Gent.